Rayleigh–Brillouin Scattering from Reacting Epoxy Resins: Comparison with Torsional Braid Analysis

SHINGO KONDO, TAKASHI IGARASHI, and TSUTOMU NAKAMURA,
Research Institute of Composite Materials, Faculty of Technology, Gunma University, Kiryu 376, Japan

Synopsis

The rheological study for isothermal curing processes of two kinds of epoxy/amine systems made by Rayleigh–Brillouin spectroscopy was compared with torsional braid analysis. The Brillouin shift increased with the increase in the density during the process. The intensity ratio of Rayleigh line to Brillouin lines (LP ratio) increased remarkably in accordance with the onset of gelation measured by extraction. The increase of scattered light suggests that some kind of density fluctuation of the order of the light wavelength takes place prior to the gelation. The longitudinal elastic modulus and the attenuation of sound in the hypersonic region changed monotonically from the start of measurement and almost leveled off after the transition to the glassy state determined by dilatometry. While the relative shear modulus in a low-frequency region ($0.1 \sim 1$ Hz) was not sensitive to the onset of gelation, it was markedly affected by the approach to the glassy state.

INTRODUCTION

Flexural braid analysis (FBA) and torsional braid analysis (TBA) are convenient methods for following the change in viscoelasticity of thermosetting resins during cure. Lewis,[1] Babayevsky and Gillham,[2] and Igarashi et al.[3] suggested that elastic moduli and damping factors in a low-frequency region were affected by "gelation" and "vitrification" in epoxy/amine systems during isothermal curing. The formation of macrostructures[4–7] during cure of thermosetting resins is important in reaction mechanisms and physical properties of cured resins. However, FBA and TBA methods do not determine the structural changes associated with gelation or vitrification.

In a recent study of the polymerization of styrene,[8] Rayleigh–Brillouin spectroscopy has been regarded as an effective method for observing the change in physical properties of chemically reactive systems. Indeed, Rayleigh–Brillouin scattering[9] reveals changes due to density fluctuations and much more information about structural changes than FBA and TBA. This includes the Rayleigh line width, the frequency shift, and the line width of the Brillouin doublet, the intensity ratio of Rayleigh line to Brillouin lines (LP ratio), and the depolarization. However, little is known about Rayleigh–Brillouin lines of chemically reacting systems.

The curing processes of two kinds of epoxy/amine systems were investigated by Rayleigh–Brillouin spectroscopy and TBA in the present study. To find the behavior of the scattered light spectra at gelation and vitrification of the reacting systems, the gel fraction and the glass transition temperature of the chemically reacting systems were measured. The behavior of elastic moduli in the hypersonic and low-frequency regions is discussed in connection with the energy and the entropy elasticities.

Journal of Applied Polymer Science, Vol. 26, 2337–2346 (1981)
 CCC 0021-8995/81/072337-10$01.00

EXPERIMENTAL

In isothermal curing processes, the preparation of samples, and the measurements were conducted at 25°C. Reaction times were started at mixing of the materials.

Materials

The following materials are used:

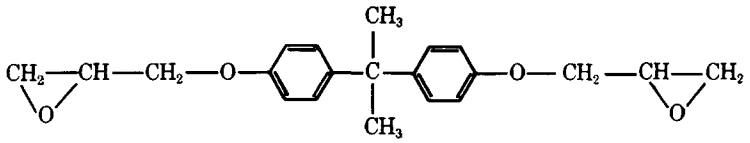

diglycidyl ether of bisphenol A (Shell Epicote-828)

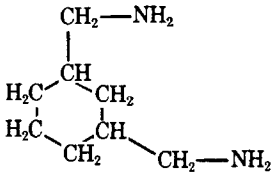

1,3-bisaminomethylcyclohexane

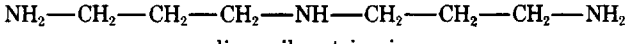

dipropilenetriamine

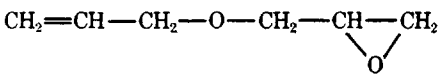

allyl glycidyl ether

One epoxy/amine system (EPBAC) is composed of diglycidyl ether of bisphenol A (100 parts), 1,3-bisaminomethylcyclohexane (17 parts), and allyl glycidyl ether (12 parts). The other epoxy/amine system (EPDPTA) is made up of diglycidyl ether of bisphenol A (100 parts), dipropilenetriamine (13 parts), and allyl glycidyl ether (12 parts). Both systems are prepared to react slowly and to have low viscosity in preparation. These systems are not stoichiometric mixtures (1 mol epoxy with 0.76 mol amine hydrogen in EPBAC and 1 mol epoxy with 0.79 mol amine hydrogen in EPDPTA). They contain the reacting diluent allyl glycidyl ether which becomes a pendent chain after reaction.

Rayleigh–Brillouin Scattering

All the reacting mixtures are filtered through a membrane (0.2 μm pore). The reacting mixture is put in a glass cell placed in an air bath at 25 ± 0.8°C. Light scattering spectrometer data was reported in a previous paper.[10] Polarized monochromatic light (wavelength of 6328 Å) is focused on the sample. The light scattered at 90 ± 1° is analyzed with a piezoelectrically scanned Fabry–Perot interferometer with a free spectral range of 30 GHz. The observation of the spectrum is made in single sweep (about 10 s) of the interferometer.

The velocity of sound v_s is calculated from the frequency shift ν_B of the Brillouin peaks:

$$v_s = \frac{\lambda_0 \nu_B}{2n_r \sin(\theta/2)} \tag{1}$$

where λ_0 is the wavelength of the incident light in vacuo, n_r is the refractive index of the scattering medium, and θ is the scattering angle. The longitudinal elastic modulus M of the medium is obtained as

$$M \equiv K + \frac{4}{3}G = \rho {v_s}^2 \tag{2}$$

where K is the bulk modulus, G is the shear modulus, and ρ is the density. Provided that observed Brillouin lines have a Lorentzian profile and that the amplitude of the sound wave damps according to exp $(-\Gamma t)$ in time and exp $(-\alpha r)$ in space, the attenuation of the hypersonic sound per cycle, $\alpha\lambda_s$ (λ_s is the wave length of sound) is estimated from a half-width at half-height Δ_B,

$$\alpha\lambda_s = \frac{\Gamma}{\nu_B} = \frac{2\pi\Delta_B}{\nu_B} \tag{3}$$

where Δ_B is obtained[11] from the observed half-width $(\Delta_B)_{\text{obs}}$ and the instrumental half-width Δ_I:

$$\Delta_B = (\Delta_B)_{\text{obs}} - \Delta_I \tag{4}$$

Torsional Braid Analysis

A Rhesca model RD-1100AD viscoelastometer was used as the torsional braid apparatus. The frequency and the amplitudes of a torsional pendulum were measured. A torsional pendulum is composed of a steel wire (0.3 mm in diameter and 100 mm in length) suspending the inertia wheel (moment of inertia of 3.4 $\times 10^3$g·cm^2) and a glass braid (1 mm in diameter and 100 mm in length) impregnated with reacting mixture and attached under the inertia wheel. The torsional pendulum is set in nitrogen gas controlled to 25 ± 0.5°C.

The relative shear modulus G_r of the sample is calculated from the frequencies:

$$G_r = \frac{\nu^2}{{\nu_0}^2} \tag{5}$$

where ν_0 is the frequency in the initial stage of measurement. The logarithmic decrement λ is obtained from the ratio of two adjacent amplitudes

$$\lambda = \ln(A_1/A_2) \tag{6}$$

where A_1 is any amplitude and A_2 is the next amplitude.

Gel Fraction

Uncrosslinked components of a reacting mixture cured in nitrogen gas controlled to 25 ± 0.8°C are extracted with methyl ethyl ketone and the insoluble components are weighed after drying. The gel fraction is obtained as the ratio of the weight of the insoluble components to the weight of the total mixture.

The reaction mechanisms of epoxy systems are complicated, and this makes the theoretical treatment of the gel fraction difficult.[12] Therefore, the theoretical estimations are not included in this study.

Density and Glass Transition Temperature During Reaction

The volume changes for reacting mixtures are measured with a mercury dilatometer. The reacting mixture (1 g) is enclosed in a rubber membrane (0.1 mm thick) and is put in a mercury dilatometer controlled to 25 ± 0.1°C. The changes in the density during isothermal curing are obtained from the volume changes.

Each sample prepared for T_g measurement is enclosed in a rubber membrane and put in a mercury dilatometer controlled at 25 ± 0.1°C; then it is cooled rapidly to −20°C from which point a temperature rise is used to measure the dilatation. The glass transition temperature is obtained as the temperature at which the coefficients of thermal expansion show a discontinuity in the specific volume-versus-temperature curve.

RESULTS

During isothermal curing of the epoxy resins at 25°C, both systems change their fluidity from the liquid to the solid state. Accordingly, the observed values of the Brillouin shift increased markedly: 7.4 GHz at 1 h, 9.6 GHz at 11 h for EPBAC [Fig. 1(a)], and 7.3 Ghz at 1 h, 9.9 GHz at 11 h for EPDPTA [Fig. 2(a)]. The elastic modulus M in the hypersonic region calculated from the above values showed a remarkable increase from the start of measurement to 13 h and then remained almost constant [Figs. 1(b) and 2(b)]. The hypersonic sound attenuation per cycle, $\alpha\lambda_s$, decreased monotonically and reached a final level in both

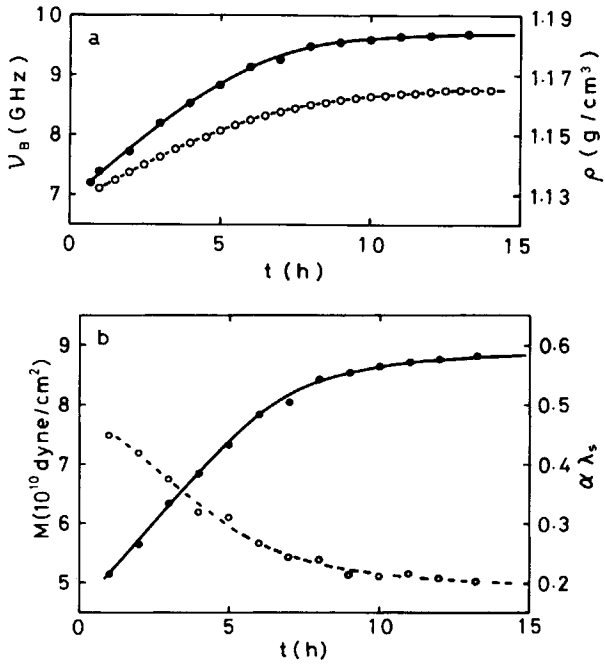

Fig. 1. Measured quantities for EPBAC as functions of reaction time: (a) The Brillouin shift ν_B (●) and the density ρ (○); (b) the longitudinal elastic modulus M (●) and the attenuation of the hypersonic sound $\alpha\lambda_s$ (○); (c) the gel fraction (●) and the intensity ratio $I_c/2I_B$ (○); (d) the relative shear modulus G_r (●) and the logarithmic decrement λ (○); (e) the glass transition temperatures T_{g+} (●) and T_{g-} (○).

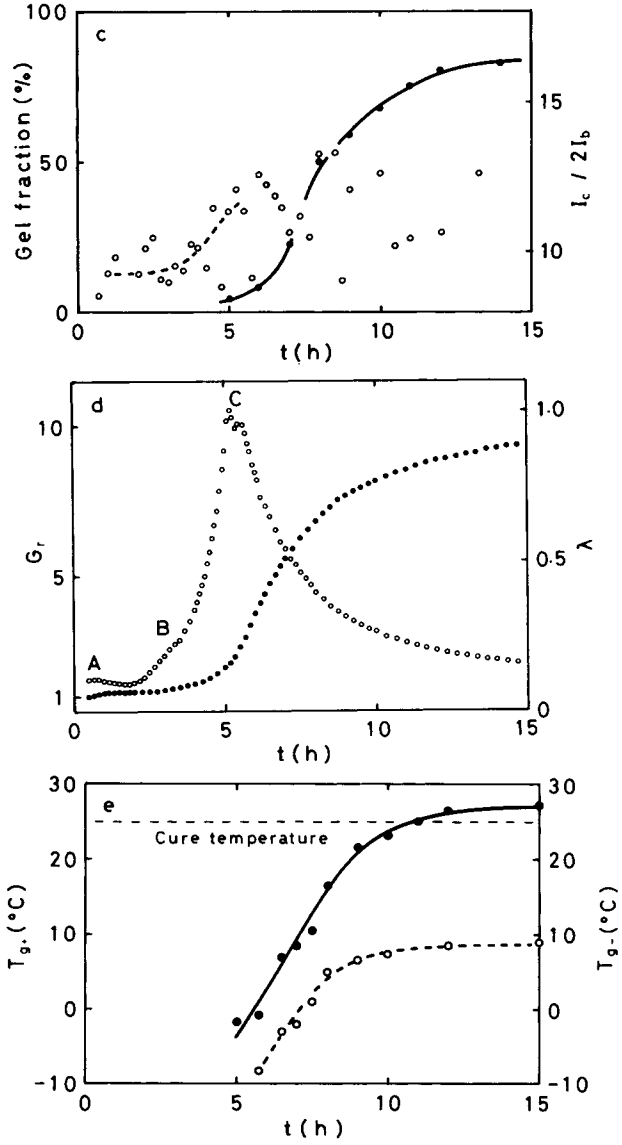

Fig. 1. (*Continued from previous page.*)

epoxy systems at about 13 h [Figs. 1(b) and 2(b)]. The intensity of Rayleigh component I_c was high in comparison with the intensity of Brillouin components $2I_B$ throughout the whole process (Fig. 3). The intensity ratio $I_c/2I_B$ rose at 4 h for EPBAC and at 3 h for EPDPTA [Figs. 1(c) and 2(c)]. Then the "speckle patterns" became conspicuous in the path of light, and after 8 h the values of $I_c/2I_B$ distributed desultorily.

The relative shear modulus G_r and the logarithmic decrement λ as functions of reaction time are shown in Fig. 1(d) for EPBAC and in Fig. 2(d) for EPDPTA. The modulus G_r showed two distinct increases. The first increase, which was accompanied by a damping peak A, started at about 1 h in both systems. One shoulder B and a peak C of damping went along with the second increase starting at 3 h in EPBAC and 4 h in EPDPTA.

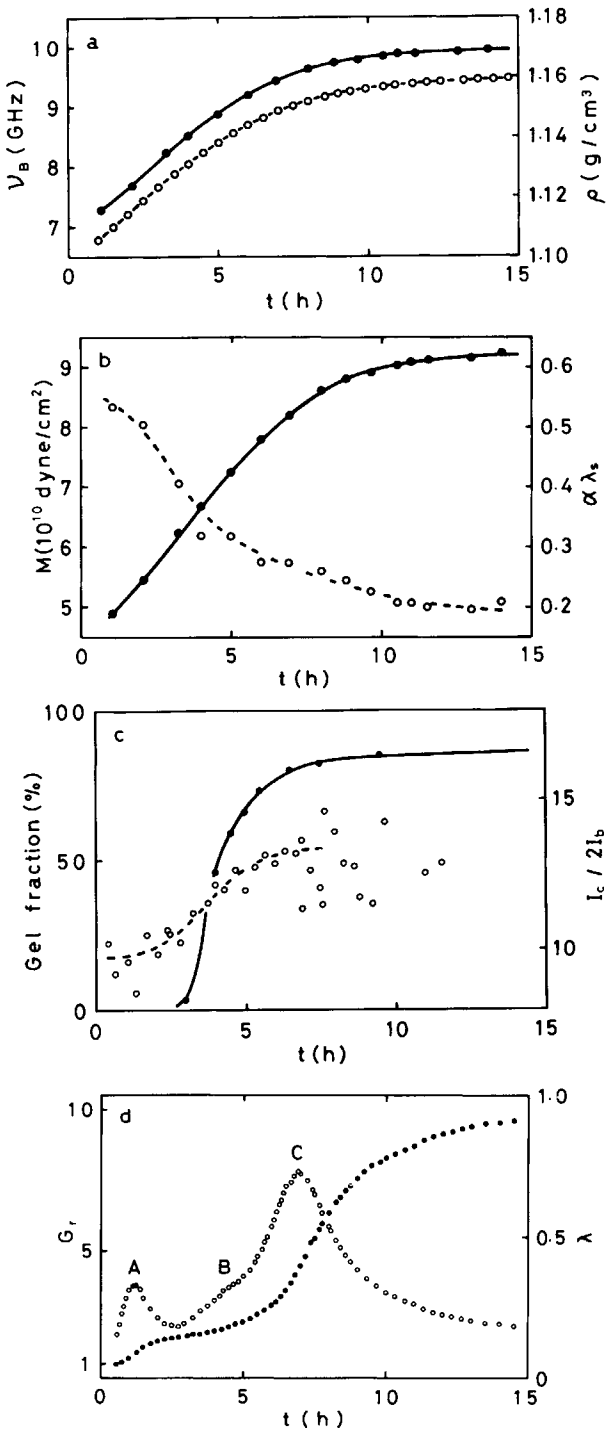

Fig. 2. Measured quantities for EPDPTA as functions of reaction time: (a) The Brillouin shift ν_B (●) and the density ρ (○); (b) the longitudinal elastic modulus M (●) and the attenuation of the hypersonic sound $\alpha\lambda_s$ (○); (c) the gel fraction (●) and the intensity ratio $I_c/2I_B$ (○); (d) the relative shear modulus G_r (●) and the logarithmic decrement λ (○); (e) the glass transition temperatures T_{g+} (●) and T_{g-} (○).

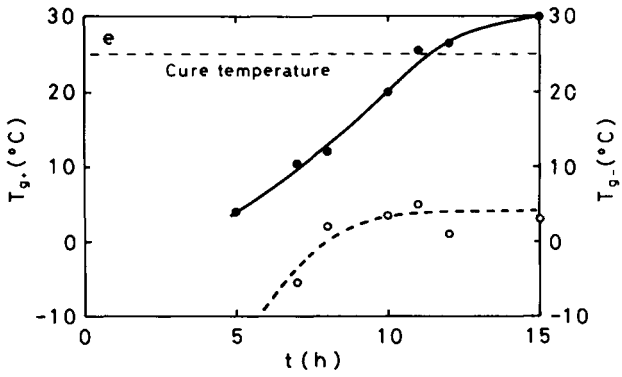

Fig. 2. (*Continued from previous page.*)

The gel fraction for EPBAC could be detected after 5 h and reached the final level near 14 h [Fig. 1(c)], while the gel fraction of EPDPTA could be detected after 3 h and extended to almost the final level at 9.5 h [Fig. 2(c)]. Soluble but gellike components could be observed for both epoxy systems prior to the detection of the gel fraction by extraction. When methyl ethyl ketone was added to the sample in this stage, it swelled by absorbing the solvent and then dissolved.

The density as a function of reaction time increased remarkably from the start of measurement to 12 h for both resins [Figs. 1(a) and 2(a)]. The specific volume–temperature curves obtained for the reacting samples changed their slope at two points of temperature (Fig. 4). The lower and higher bending temperatures were denoted by T_{g-} and T_{g+}, respectively. As the reaction proceeded, the difference between T_{g-} and T_{g+} became larger. The value of T_{g+} was −2°C at 5 h and 25°C at 11 h for EPBAC [Fig. 1(e)] and was 4°C at 5 h and 25°C at 11.5 h for EPDPTA [Fig. 2(e)]. When the observed value of T_{g+} arrived at the reaction temperature, the hardness of the reacting resin showed a marked increase

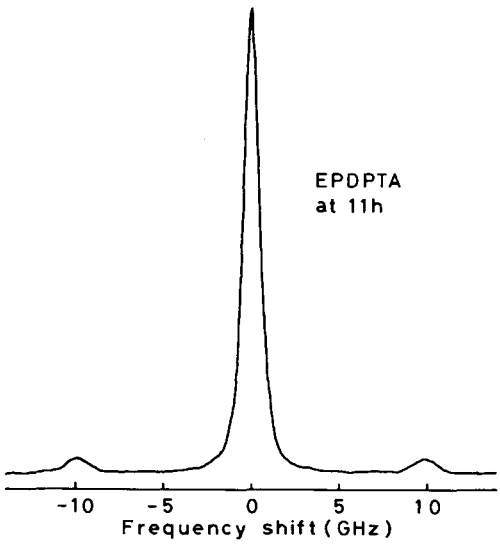

Fig. 3. Rayleigh–Brillouin spectra for EPDPTA at the reaction time of 11 h.

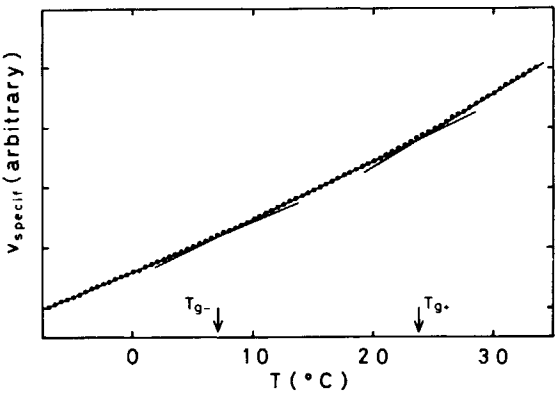

Fig. 4. Specific volume of EPBAC at the reaction time of 10 h as function of temperature. The lower and higher bending temperatures are indicated by T_{g-} and T_{g+}, respectively.

and became glassy [Figs. 1(e) and 2(e)]. T_{g+} is the glass transition temperature. It is not clear to what transition T_{g-} corresponds.

DISCUSSION

At the onset of gelation, both epoxy systems (EPBAC and EPDPTA) are in the rubbery state. When the value of the gel fraction levels off, EPBAC is in the glassy state and EPDPTA is still in the rubbery state, though EPDPTA is finally in the glassy state [Figs. 1(c), 1(e), 2(c), and 2(e)]. The relative shear modulus G_r in a low-frequency region shows a two-step increase: the first slight increase having little connection with gelation measured by extraction and vitrification determined by dilatometry; the second marked increase being affected simultaneously by gelation and vitrification [Figs. 1(c)–1(e) and 2(c)–2(e)]. The time when the shoulder appears in the logarithmic decrement curve corresponds with the time when the soluble but gellike components can be observed. On one hand, the damping peaks are located near the inflection point of the relative shear modulus curve, that is, a damping peak accompanies a sigmoidal increase in the elastic modulus. The Brillouin shift, the logitudinal elastic modulus M in the hypersonic region, and the density resemble each other in behavior during the reaction: their values are not affected by gelation measured by extraction and almost cease to increase after the transition to the glassy state, determined by dilatometry. The intensity ratio $I_c/2I_B$ as a function of the reaction time is affected by the onset of gelation and rises. Further, the appearance of "speckle patterns" and the behavior of $I_c/2I_B$ are related to each other.

The difference in behavior between the elastic moduli in the low and the hypersonic frequency regions may be attributed to frequencies used for measurements and to the mechanisms for elasticity,[10] i.e., the entropy elasticity and the energy elasticity. The moduli obtained from the Brillouin shift are related to the energy elasticity of short-range interaction in collective motion of molecules or segments. However, the increase in molecular weight and crosslink density may cause the motion of molecules with longer relaxation times and a restriction of configurational rearrangement of molecules. If configurational rearrangements occur sufficiently in the time scale of the observed frequency in the measurement of the elastic moduli, the observed elastic moduli will reflect the

entropy elasticity with energy dissipation. If they do not, the observed elastic moduli will reflect the energy elasticity. Therefore, the first and the second increases in the relative shear modulus G_r of both regions are related, respectively, with occurrence of the entropy elasticity caused mainly by entanglements of molecular chains and the energy elasticity caused by the approach to the glassy state. Since a relaxation phenomenon in the hypersonic region is observed[13,14] far above the glass transition temperature for polymeric chain molecules, the configurational rearrangement of molecular chains are severely restricted in the hypersonic time scale near the glass transition temperature. Polymeric chain molecules behave like solids in that time scale and temperature region. On the other hand, the Brillouin shift ν_B is known to be equal to the frequency of the sound wave,[9,15] i.e., phonon. The lattice theory[10,15] tells us that the frequency of sound depends on the density and force constants. The hypersonic longitudinal elastic modulus M of epoxy systems, on basis of the energy elasticity, may express the extent of reaction in the present isothermal curing.

One sigmoidal increase in G_r accompanies one damping peak, no matter what the mechanisms of elasticity. The damping peaks relate to relaxation during the isothermal curing process, though we have no precise theoretical explanation. Accordingly, the hypersonic sound attenuation decreases monotonically without going through a peak, indicating a weak participation of relaxation at gelation and vitrification.

The increase in the intensity ratio $I_c/2I_B$ as a function of temperature was discussed previously in connection with relaxation[16] and the frozen-in density fluctuations[13] or the temperature-dependent nonpropagating strains.[17] In the present case, the increase in $I_c/2I_B$ occurs in accordance with the onset of gelation, but the reacting systems are neither in relaxation nor in the glassy state. Therefore, in curing systems, the increase in the intensity ratio $I_c/2I_B$ relates to the nonuniformity of order of the light wavelength in the network structure. While the relative shear modulus does not show a stepwise increase at the onset of gelation, the damping shows a shoulderlike increase. This suggests that entanglements and crosslinks of molecular chains play similar roles for the entropy elasticity, but there is some kind of mechanism causing the energy dissipation during the process of network formation.

Rayleigh–Brillouin spectroscopy follows sensitively the behavior of density and density fluctuations in reacting systems. However, density fluctuations may not be reflected in low-frequency experiments of TBA. TBA is effective in detecting the change in the elastic modulus and the energy dissipation associated with the glass transition, but it provides little information on gelation.

The TBA method has several problems when used to estimate the properties of reacting specimens. These include the "composite effects" between the reacting mixture and the glass braid and the effects of preferential volatilization of some reactive components and of absorption of harmful environmental gases through the large surface area of TBA specimens.

References

1. A. F. Lewis, *SPE Trans.*, **3**, 201 (1963).
2. P. G. Babayevsky and J. K. Gillham, *J. Appl. Polym. Sci.*, **17**, 2067 (1973).
3. T. Igarashi, S. Kondo, and M. Kurokawa, *Polymer*, **20**, 301 (1979).
4. R. E. Cuthrell, *J. Appl. Polym. Sci.*, **11**, 949 (1967); *ibid.*, **12**, 1263 (1968).

5. K. Horie, A. Otagawa, M. Muraoka, and I. Mita, *J. Polym. Sci. Polym. Chem. Ed.*, **13,** 445 (1975).
6. K. Dusek, J. Plestil, F. Lednicky, and S. Lunak, *Polymer*, **19,** 393 (1978).
7. E. H. Erath and M. Robinson, *J. Polym. Sci., Part C*, **No. 3,** 65 (1963).
8. D. A. Jackson and J. R. Stevens, *Molc. Phys.*, **30,** 911 (1975).
9. L. D. Landau and E. M. Lifshitz, *Electrodynamics of Continuous Media*, Pergamon, Oxford, 1960.
10. S. Kondo and T. Igarashi, *J. Appl. Phys.*, **51,** 1514 (1980).
11. H. W. Leidecher, Jr., and J. T. La Macchia, *J. Acoust. Soc. Am.*, **43,** 143 (1967).
12. P. Flory, *Principles of Polymer Chemistry*, Cornell University Press, Ithaca, N. Y., 1953.
13. Y. Y. Huang and C. H. Wang, *J. Chem. Phys.*, **62,** 120 (1975).
14. G. D. Patterson, *J. Polym. Sci. Polym. Phys. Eds.*, **15,** 455 (1977).
15. C. Kittel, *Introduction to Solid State Physics*, Wiley, New York, 1971.
16. D. A. Pinnow, S. J. Candau, J. T. La Macchia, and T. A. Litovitz, *J. Acoust. Soc. Am.*, **43,** 131 (1967).
17. J. R. Stevens, I. C. Bowell, and J. L. Hunt, *J. Appl. Phys.*, **43,** 4354 (1972).

Received March 25, 1980
Accepted January 9, 1981